Effect of Depth on the Pattern Formation of Faraday Waves

Doug Binks, Mark-Tiele Westra, and Willem van de Water
Physics Department, Eindhoven University of Technology, P.O. Box 513, 5600 MB, Eindhoven, The Netherlands
(Received 9 July 1997)

The symmetry of standing wave patterns on the surface of a vertically oscillated fluid layer depends on the depth of the layer. In a large experiment we trace out the stability diagram. The dependency can be understood on the basis of the oscillatory character of the waves and the dispersion relation. A simple amplitude equation can be constructed with the variation with depth of the dispersion relation and a general quadratic nonlinearity as its only ingredients. The predictions of this model agree well with the experiment. [S0031-9007(97)04783-2]

PACS numbers: 47.35.+i, 47.54.+r

Recently a great deal of attention has been focused on the nonlinear dynamics of parametrically excited systems, such as spin waves [1], second sound in superfluid helium [2], vertically oscillated granular layers [3], and waves on a free fluid surface undergoing oscillatory vertical acceleration (Faraday waves) [4,5]. These waves can organize in many symmetric forms, and stripes, squares, hexagons, and quasiperiodic patterns have been observed. An explanation of this pattern forming instability has been given in terms of amplitude equations which describe the slow evolution of the amplitude of waves with wave number equal to the critical wave number. As the free surface problem is one of the most difficult problems of hydrodynamics, the formulation of an amplitude equation for Faraday waves is a formidable task [6,7]. This approach has led to a prediction of pattern symmetries that is in striking agreement with experiment [6–9]. However, the theory was formulated for deep fluids and an intriguing discrepancy remains with the experimental observation of wave patterns on shallow fluid layers [8]. This encouraged us to study carefully the influence of the layer depth on the symmetry of the onset pattern. In this Letter we will show that the discrepancy can be resolved by considering the change of the dispersion relation with depth. This central role of the dispersion relation can be exploited for constructing an approximate amplitude equation whose predictions are in favorable agreement with the experiment. The agreement is surprising because the only other ingredient of our model is a general quadratic nonlinearity.

Our experimental setup is described in detail in [9]. A 440 mm diameter sealed circular container is filled to a height h (in the range 2–20 mm) with the working fluid [10]. The container is vibrated in the vertical direction by an electromagnetic exciter, with the acceleration being measured by a high-resolution piezoelectric accelerometer. The measured acceleration inhomogeneity over the plate is less than 2%, the acceleration is controlled to better than 0.2%, and the frequency to 1 part in 10^6. The waves are visualized using the shadowgraph method, and images of the surface are made using a CCD camera with a liquid crystal shutter in order to obtain images at a constant phase of the excitation. The diameter of the container is large enough that the pattern formation is insensitive to the presence of the lateral boundaries (for a discussion of the effective size of the experiment, see [9]).

The strong dependency of the symmetry of the onset pattern on the fluid layer depth is illustrated in Fig. 1, which shows the imaged surface of the fluid layer close to onset at a fixed frequency of 29 Hz, but for two different depths. The pattern at a depth of $h = 10$ mm is an eightfold quasiperiodic structure, in agreement with recent theory which was formulated in the infinite depth limit [6,7,9]. However, at a depth of $h = 3.5$ mm the pattern observed is now hexagonal, in seeming disagreement with this theory as has been previously observed [8]. In Fig. 2 we present the regions of stability of square, hexagonal, and eightfold quasiperiodic patterns as a function of depth (the lines are from theoretical descriptions which will be explained later). Both the frequencies for the square/hexagonal, and hexagonal/eightfold boundaries show a similar trend and decrease with decreasing depth [11].

One of the primary effects of changing the depth of the fluid layer is to alter the form of the dispersion relation, which to a good approximation is given by the inviscid dispersion relation $\omega_0^2(k) = \tanh(kh)[gk + (\sigma/\rho)k^3]$ where k is the wave number of the waves, g the acceleration due to gravity, σ the surface tension, and ρ the

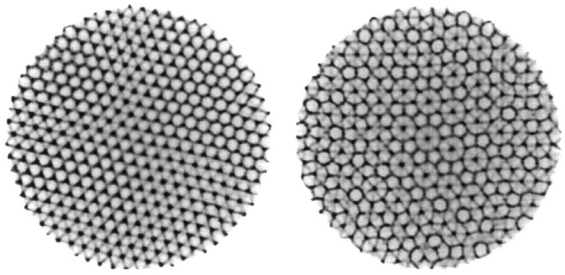

FIG. 1. Images of the surface at an excitation frequency of 29 Hz, taken just above onset, for depths of (a) 3.5 mm, showing a hexagonal pattern, and (b) 10 mm, showing an eightfold quasiperiodic pattern.

 0031-9007/97/79(25)/5010(4)$10.00

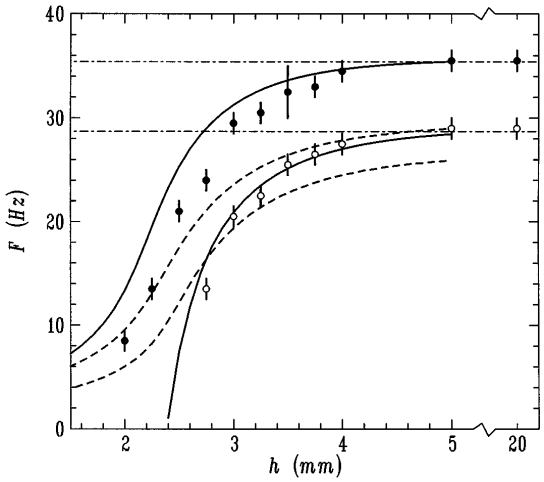

FIG. 2. Frequency boundaries between different pattern symmetries observed close to threshold as a function of the depth. Closed circles: square/hexagon boundary. Open circles: hexagon/eightfold boundary. Dash-dotted lines: predictions from [7] for infinite depth square/hexagon (upper) and hexagon/eightfold boundary (lower). Dashed lines: prediction of the stability boundaries on the basis of Eq. (2). Full lines: Contours of constant resonance angle (using the fully viscous dispersion relation) chosen such that at infinite depth they pass through the transition frequencies. The error in the depth stems mainly from the leveling accuracy. It can be estimated as ± 0.1 mm at the walls of the container.

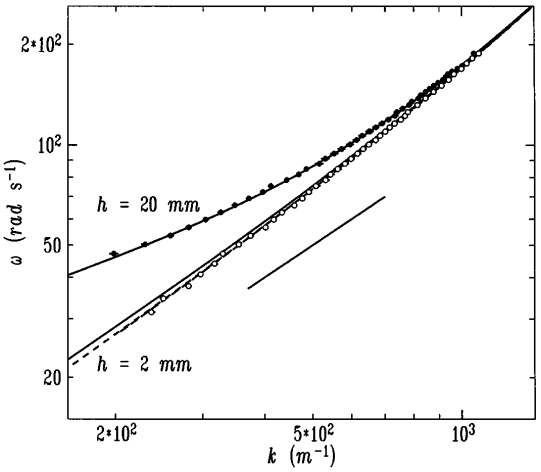

FIG. 3. Dispersion relation $\omega_0(k)$ plotted on a log-log scale. ω_0 is the angular frequency of the waves, and is calculated from $\omega_0 = \Omega/2$. Closed circles: experimentally measured points for a depth of $h = 20$ mm (effectively infinite for this range of k). Open circles: measurements for a depth of $h = 2$ mm. Solid lines: $\omega_0^2(k) = \tanh(kh)[gk + (\sigma/\rho)k^3]$ for $h = 20$ mm (upper line) and 2 mm (lower line). Dashed lines: viscous theory [12,13] for $h = 20$ mm (the line corresponding to $h = 20$ mm is not visible as it coincides with the solid line), and 2 mm (lower line). The short line segment designates the linear dependence $\omega \propto k$.

density of the fluid. Parametrically excited systems typically undergo a bifurcation to a standing wave state where the frequency and wave number of the waves is determined by (but not necessarily equal to) the frequency and wave number of the excitation. The excitation wave with frequency Ω decays into two waves at ω_1 and ω_2 following the rule $\Omega = \pm(\omega_1 - \omega_2)$. In most cases the surface responds subharmonically with $\omega_1 = -\omega_2 = \Omega/2$, and the wave number k_c is given by the dispersion relation with $\omega_0(k) = \Omega/2$. Harmonic waves have higher dissipation, and thus the initial bifurcation is to subharmonic waves. However, with thin fluid layers harmonic waves have recently been predicted and observed [12]. Figure 3 shows the wave number measured close to onset as a function of the frequency of the waves for depths of 20 and 2 mm. In addition, we have plotted the inviscid dispersion relation, and the viscous dispersion relation from the full stability analysis [12,13]. The inviscid dispersion relation agrees well with both experiment and viscous theory, although the viscous theory gives a better prediction of the data at 2 mm. Because the thickness of the viscous boundary layer is much smaller than the depth, almost all viscous damping takes place in the bulk of the fluid.

In addition to the waves generated by interaction with the excitation, waves can be generated by nonlinear interactions in which the dispersion relation plays a significant role. As wave amplitudes are small, quadratic and cubic nonlinearities dominate. When Fourier transformed into $\mathbf{k}, \omega$ space, quadratic nonlinearities lead to three wave (3W), and cubic to four wave (4W) interactions. If all of the waves in any given interaction have wave numbers and frequencies that satisfy the dispersion relation, then these waves will be resonant, and thus the interaction will be amplified considerably in comparison to that not involving resonant waves. While resonant 4W interactions can always be found for a given dispersion relation, resonant 3W interactions only exist when $\omega \propto k^p$ where $p > 1$ (termed *decay type* dispersion relations). This is indeed the case for infinite depth inviscid capillary waves ($\omega \propto k^{3/2}$) but not for gravity waves ($\omega \propto k^{1/2}$). This has been shown to have a great effect on the pattern formation of Faraday waves [6,7,9]. Thus, one expects that if the dispersion relation is altered, the regions of different pattern symmetries will alter accordingly. In Fig. 3 we have plotted the line corresponding to $\omega \propto k$ with the experimental results. Dispersion relations with a steeper gradient will be of decay type and so support resonant 3W interactions, as described above. It can thus be seen that while the dispersion relation for 20 mm is of decay type for high ω, it is nondecay for low ω. The dispersion relation for 2 mm, however, is of decay type throughout the displayed frequency region. The stable pattern regions in Fig. 2 all lie in a frequency range where the dispersion relation is of decay type, and we thus expect 3W interactions to predominate.

Three-wave interactions are the result of quadratic nonlinearities. Let us briefly sketch how such interactions arise. A quadratic nonlinearity in the surface height ζ will spawn waves with wave vector $\mathbf{k}_3$ from waves with $\mathbf{k}_1$

and $\mathbf{k}_2$. The amplitude $\zeta_{\mathbf{k}_3}$ obeys a wave equation with quadratic nonlinearity

$$\ddot{\zeta}_{\mathbf{k}_3} + \mu(k_3)\dot{\zeta}_{\mathbf{k}_3} + \omega_0^2(k_3)\zeta_{\mathbf{k}_3} = \int_{\mathbf{k}_1+\mathbf{k}_2=\mathbf{k}_3} d\mathbf{k}_1\, d\mathbf{k}_2\,, \qquad (1)$$

where $\mu(k)$ provides damping. In Eq. (1) we have ignored the direct excitation and omitted a prefactor of the quadratic coupling term. As will be explained in a longer write-up, the wave vector dependence of this prefactor is not essential for our model. For weakly viscous waves the damping can be approximated by $\mu(k) = 4\nu k^2$ with ν the viscosity. Close to onset, the surface waves $\mathbf{k}_1, \mathbf{k}_2$ have frequency $\omega = \Omega/2$ and wave number $|\mathbf{k}_1| = |\mathbf{k}_2| = k_c$ that satisfies the dispersion relation $\omega_0(k_c) = \Omega/2$.

The nonlinearly produced waves $\mathbf{k}_3$ are at frequency Ω and do not in general satisfy the dispersion relation. A special case is when the angle θ between $\mathbf{k}_1$ and $\mathbf{k}_2$ is such that $k_3 = 2\cos(\theta/2)k_c$ *does* satisfy the dispersion relation $\omega_0(k_3) = \Omega$. Because the wave $\mathbf{k}_3$ is strongly damped [when resonant, $k_3 > k_c$, and thus $\mu(k_3) > \mu(k_c)$], patterns with wave vectors that have mutual angles close to the resonance angle θ_r, with $\omega_0[2\cos(\theta_r/2)k_c] = \Omega$, will not be preferred. In fluids of infinite depth, the resonance angle decreases from $\theta_r \approx 74.9°$ at high frequencies to $\theta_r = 0°$ at $\omega = 85.22\ \mathrm{rad\,s^{-1}}$. Below this frequency, 3W interactions cannot be resonant (though they still exist). In Fig. 4 we plot θ_r as a function of frequency for depths between infinite and 2 mm. With decreasing depth, the resonance angle increases and the frequency at which $\theta_r = 0$ decreases.

The nonlinearly produced waves $\mathbf{k}_3$ will couple through a quadratic interaction with the directly excited waves to provide an effective damping which is then third order in the amplitude. Thus, pattern formation is a balance between this nonlinear damping and the energy input from parametric excitation. The growth and saturation of the amplitude of directly excited waves can thus be described by an amplitude equation which consequently has a third-order nonlinear saturation term

$$\dot{A}_i = \varepsilon A_i - \sum_j [\beta(\theta_{ij}) + \beta(\pi - \theta_{ij})]A_j^2 A_i\,, \qquad (2)$$

where A_i is the amplitude of wave $\mathbf{k}_i$, and ε is the reduced excitation amplitude $\varepsilon = (a - a_c)/a_c$ with a_c the critical amplitude where waves first appear. The coupling function $\beta(\theta_{ij})$ in Eq. (2) depends on the angle θ_{ij} between the wave vectors $\mathbf{k}_i$ and $\mathbf{k}_j$. An approximate coupling function follows immediately from Eq. (1)

$$\beta(\theta) = \frac{\mu(k)}{[\omega_0^2(k) - \Omega^2]^2 + \Omega^2\mu^2(k)}\,, \quad \text{with } k = 2\cos(\theta/2)k_c\,, \qquad (3)$$

where we note that $\beta(\theta = 0) = \beta(\theta \to 0)/2$ as the integral over $\mathbf{k}_1$ and $\mathbf{k}_2$ leads to two interactions when $\theta \neq 0$. Our approximation of $\beta(\theta)$ is crude, in that it assumes an arbitrary quadratic nonlinearity and omits cubic terms which lead to 4W interactions. A precise derivation of $\beta(\theta)$ is only possible in a full hydrodynamic approach, as has been performed in [6,7]; however, we will demonstrate that our $\beta(\theta)$ contains the essential physics of pattern formation.

The coupling function $\beta(\theta)$ displays a resonance phenomenon. Figure 5 illustrates how the resonance peaks shift with fluid depth. As is well known, the presence of this resonance is of key importance for pattern formation [6], and we will demonstrate that the change of pattern symmetry with depth is governed by the corresponding change of the resonance peaks. Equation (2) is of gradient form and a Lyapunov functional (or free

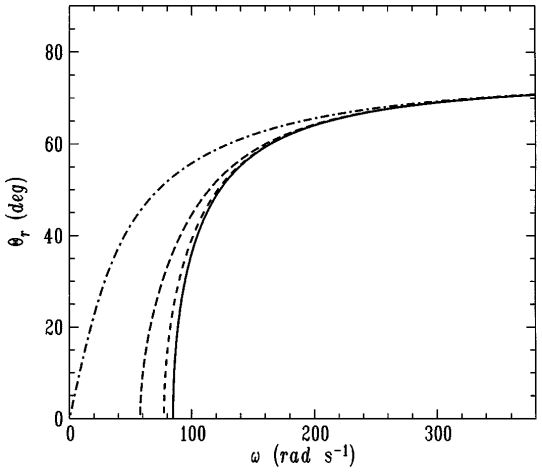

FIG. 4. Resonant angle θ_r as a function of frequency ω for depths of 20 mm (solid line), 4 mm (short-dashed line), 3 mm (long-dashed line), and 2 mm (dot-dashed line).

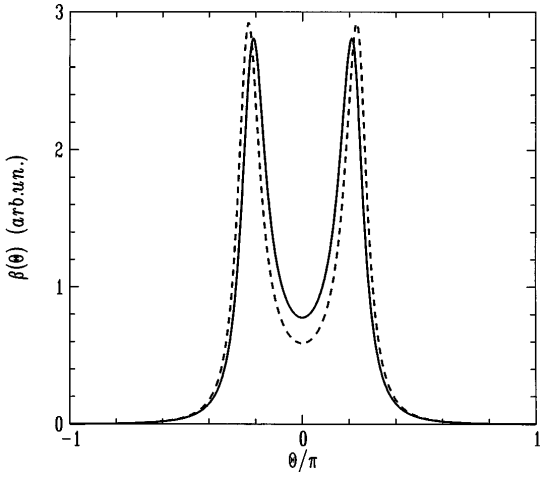

FIG. 5. Approximate coupling function $\beta(\theta)$ for a wave number of 600 $\mathrm{m^{-1}}$. Full line: depth $h = 10$ mm; dashed line: $h = 3.5$ mm.

energy) can be defined. The preferred onset pattern is the one that minimizes the Lyapunov functional. This calculation leads to the predicted boundaries for the square to hexagonal (2−3 wave), and hexagonal to eightfold (3−4 wave) pattern symmetries, which are plotted in Fig. 2. For such a simplified theoretical description, containing only the essential changes to the dispersion relation and an arbitary quadratic interaction, the *quantitative* agreement is surprisingly good. As only the dispersion relation contains any depth dependence in this model, its importance to pattern formation is clearly illustrated.

An intriguing observation is that transitions lie approximately on lines of constant resonance angle. Using the fully viscous dispersion relation, we have plotted two lines of constant resonance angle in Fig. 2 which were chosen so as to go through the transition frequencies at 20 mm. While this is not an absolute comparison, the relative dependence on h is extremely close to that of the pattern transitions.

That resonant angles are avoided in these patterns is fortunate for their description in terms of amplitude equations. If resonant interactions are present, the resonantly produced wave may grow in amplitude to the same order of magnitude as the parametrically excited waves, and thus contribute significantly to the nonlinearity. An amplitude type equation cannot then be formulated, as these equations only describe the dynamics of the linearly unstable wave vectors assuming the nonlinearly produced waves to be of a small enough amplitude for their own nonlinear terms to be insignificant.

In conclusion, by making explicit use of the oscillatory nature of Faraday waves, together with the associated dispersion relation, we have formulated a remarkably simple explanation of the change of pattern symmetries with depth. We believe that our route gives a better approach to constructing models of this pattern forming instability than a start from generic amplitude equations [14].

We thank Gerard Trines for technical assistance, and Eric Bosch, Hanns Walter Müller, Laurette Tuckerman, and Christian Wagner for many useful discussions. We gratefully acknowledge financial support by the "Nederlandse Organisatie voor Wetenschappelijk Onderzoek (NWO)" and "Stichting Fundamenteel Onderzoek der Materie (FOM)."

[1] V. S. L'vov, *Wave Turbulence under Parametric Excitation* (Springer-Verlag, Berlin, 1994).
[2] D. Rinberg, V. Cherepanov, and V. Steinberg, Phys. Rev. Lett. **76**, 2105 (1996).
[3] F. Melo, P. Umbanhowar, and H. L. Swinney, Phys. Rev. Lett. **74**, 4643 (1995).
[4] M. Faraday, Phil. Trans. R. Soc. London **121**, 319 (1831).
[5] M. C. Cross and P. Hohenberg, Rev. Mod. Phys. **65**, 851 (1993).
[6] W. Zhang and J. Viñals, Phys. Rev. E **53**, R4283 (1996); W. Zhang and J. Viñals, J. Fluid Mech. **336**, 301 (1997).
[7] P. Chen and J. Viñals, Phys. Rev. Lett. **79**, 2670 (1997).
[8] A. Kudrolli and J. P. Gollub, Physica (Amsterdam) **97D**, 133 (1996).
[9] D. Binks and W. van de Water, Phys. Rev. Lett. **78**, 4043 (1997).
[10] The working fluid is temperature controlled at $21.00 \pm 0.05\,^{\circ}\mathrm{C}$. The fluid is a low viscosity, low surface tension silicon oil with (at $21.0\,^{\circ}\mathrm{C}$) viscosity $\nu = 3.397 \times 10^{-6}\ \mathrm{m^2\,s^{-1}}$, density $\rho = 892.4\ \mathrm{kg\,m^{-3}}$, and surface tension $\alpha = 18.3 \times 10^{-3}\ \mathrm{J\,m^{-2}}$. The tendencies of the parameters with temperature are such that they are constant to within 0.1%.
[11] The stability boundaries of the patterns were determined by very slowly increasing the excitation amplitude and registering the pattern at $\epsilon = 0.1$. Just at onset ($\epsilon = 0$), the effective size of the experiment is very small, and only Bessel modes can be observed [9]. In a few cases there is a range of frequencies where a mixed mode is observed. This range is the size of the error bars in Fig. 2.
[12] H. W. Müller, H. Wittmer, C. Wagner, J. Albers, and K. Knorr, Phys. Rev. Lett. **78**, 2357 (1997).
[13] K. Kumar and L. S. Tuckerman, J. Fluid Mech. **279**, 49 (1994).
[14] H. W. Müller, Phys. Rev. E **49**, 1273 (1994).